Satellites, Oceanography and Society
edited by David Halpern

Chapter 3

ECMWF wave modeling and satellite altimeter wave data

Peter Janssen
European Centre for Medium-Range Weather Forecasts, Reading, United Kingdom

Abstract. Satellite altimeter wave height data have important benefits to society: ship routing, fisheries, coastal protection, oil exploration, specification of initial sea state for ocean wave forecasting, and validation of wave forecast. This presentation briefly describes the role of altimeter data in modern ocean wave forecasting. Also, some assumptions to obtain wave height from the radar backscattered pulse are discussed. Comparison of European Remote-sensing Satellite (ERS-2) altimeter wave height data with buoy observations revealed that the ERS-2 wave height is too low by about 7%. The underestimation is discussed and, by using model wave spectra, a method is proposed to remove this problem.

1. Introduction

Sea state forecasting started more than fifty years ago when there was a need for knowing the wave state during sea-land operations in the Second World War. The past five decades have seen ocean wave forecasting develop from simple manual techniques to sophisticated numerical wave models based on physical principles. In the 1990s, development was rapid because of availability of wave data from satellites such as geodetic satellite (Geosat), European Remote-sensing Satellite (ERS-1 and ERS-2), and Topography Experiment (TOPEX)/Poseidon, named T/P. In the mid-1980s, there was a convergence of the need to improve wave modeling, availability of powerful computers, and prospects for remote sensing techniques to provide sea state data on a global scale (SWAMP 1985). As a consequence, a group of mainly European wave modelers, who called themselves the Wave Model (WAM) group, started to develop a surface wave model from first principles, i.e., a model that solves the energy balance equation for surface gravity waves. The source functions in the energy balance included an explicit representation of wind input, nonlinear interactions, and dissipation by white capping. WAMDI (1988) describes the first version of this new wave model, called WAM.

The quality of the initial WAM was evaluated with SeaSat (Janssen et al. 1989; Bauer et al. 1992) and Geosat (Romeiser 1993) altimeter wave height data. Also, WAM has been validated against buoy data (Zambresky 1989; Wittman et al. 1995; Khandekar and Lalbeharry 1996; Janssen et al. 1997b). Modeled wave heights obtained by forcing WAM with European Centre for Medium-Range Weather Forecasts (ECMWF) winds showed good agreement with altimeter wave heights, but there were also considerable regional and seasonal differences. During the Southern Hemisphere winter, WAM underestimated wave height by about 20% in large parts of the Southern Hemisphere and in the tropical regions. The discrepancies could be ascribed to shortcomings in WAM physics and ECMWF wind fields, which at the end of the 1980s were too low in the Southern Hemisphere because of a fairly low-resolution (T106) atmospheric general circulation model. WAM contained too much dissipation of swell and a weak wind input source function.

In November 1991, the next version of WAM, named WAM cy4 (Janssen 1991; Komen et al. 1994), became part of the ECMWF wave prediction system. In addition, in September 1991 the horizontal and vertical resolutions of the ECMWF atmospheric general circulation model were doubled to produce a better representation of surface winds, in particular for the Southern Ocean. Therefore, in late 1991 there was sufficient confidence in the quality of the ECMWF wind-wave forecasting system that it could be used for the validation of ERS-1 altimeter wind and wave products. ERS-1 was launched in July 1991. Comparison of ERS altimeter wind and wave products with corresponding ECMWF fields identified problems in the ERS wind speed and wave height retrieval algorithms (Hansen and Guenther 1992; Janssen et al. 1997a).

In August 1993, assimilation of ERS-1 altimeter wave heights was introduced into the ECMWF wave forecasting system (Janssen et al. 1989; Lionello et al. 1992), which led to an improved wave analysis (Bauer and Staabs 1998). However, the ECMWF wave height analysis was too low by about 25 cm compared to buoy data because the ERS altimeter underestimated wave height by 15% (Janssen et al. 1997a).

This paper shows how comparisons of satellite altimeter wave height and wind speed data with corresponding data products computed from the ECMWF wave forecasting system have benefited both satellite observations and numerical model simulations of surface waves.

2. Surface Wave Modeling and Prediction

2.1 Brief history

Interest in surface wave prediction started during the Second World War because of the practical need for knowledge of the sea state during amphibious operations. The first predictions were based on the work of Sverdrup and Munk (1947), who used empirical relations to predict windsea and swell. An important step forwards was the introduction

of the concept of a wave spectrum (Pierson et al. 1955), but a dynamical equation describing the evolution of the spectrum was not known until Gelci et al. (1957) introduced the spectral transport equation. However, Gelci et al. (1957) used an empirically-derived net source function to describe the rate of change of the wave spectrum. The Phillips (1957) and Miles (1957) new theories of wave generation by wind and Hasselmann's (1962) development of the source function for nonlinear transfer of energy between waves provided the ingredients for the source function analytical model, consisting of input from wind, nonlinear transfer, and dissipation by white capping. For deep-water waves, the mathematical form is still used today.

None of the wave models developed in the 1960s and 1970s computed the wave spectrum from the full energy balance equation. Additional ad-hoc assumptions were introduced to ensure that the wave spectrum complies with preconceived notions of wave development that were in some cases not consistent with the source functions. Reasons for introducing simplifications in the energy balance equation were twofold: the important role of wave-wave interactions in wave evolution was not recognized; and limited computer power precluded the use of nonlinear transfer in the energy balance equation.

The relative importance of nonlinear transfer and wind input became evident from experiments on wave growth (Mitsuyasu 1968, 1969; Hasselmann et al. 1973) and from direct measurements of wind input to waves (Snyder et al. 1981). Eventually, this led in the 1980s, with availability of powerful computers, to the development of a wave prediction model that yielded the wave spectrum by integration of the energy balance equation without any prior restriction on spectral shape. Denoting the two-dimensional frequency (f)-direction (θ) wave variance spectrum by $F(f,\theta)$, the time rate of change of the wave spectrum is derived from the energy balance equation for deep-water surface gravity waves,

$$\frac{\partial}{\partial t}F + \mathbf{v}_g \bullet \nabla F = S_{in} + S_{nl} + S_{ds} \tag{1}$$

where $\mathbf{v}_g$ is the group velocity, and the source functions on the right side of equation (1) are the rates of change of the wave spectrum by wind input (S_{in}), nonlinear four wave interactions (S_{nl}), and dissipation by white capping (S_{ds}).

In the present version of WAM, the wind input is based on a parameterization of the Miles (1957) instability, including feedback of growing waves on the wind profile (Janssen 1989, 1991). As a result, the airflow drag over the ocean is sea-state dependent, in agreement with observations (Donelan 1982; Smith et al. 1992; Donelan et al. 1993; Johnson et al. 1998). A sea-state dependent drag may have consequences for the atmospheric climate (Janssen and Viterbo 1996). However, whether sea state has a significant influence on the drag coefficient remains an ongoing debate. For a pure windsea, Donelan et al. (1993) find a relation between the enhancement of the drag coefficient and a measure for the sea state, namely the wave age; however, alternatives to the wave age parameter

exist (Monbaliu 1994; Anctil and Donelan 1996; Janssen 1997). In general, the sea state is confused, consisting of a mixture of windsea and swell and, therefore, a characterization of sea state in terms of wave age is not a viable option. For example, Yelland et al. (1998) could not detect a wave age dependence of the drag coefficient for the open ocean. However, Hare et al. (1999) did find indications of a sea-state dependence of the drag coefficient because the Charnock parameter increased with increasing wind speed.

Phillips (1960) and Hasselmann (1962) showed that resonant energy transfer among four surface waves, or nonlinear wave-wave interactions, is an important component to determine the shape of the wave spectrum. Nonlinear transfer of energy also plays a vital role in shifting the spectrum towards lower frequency (Hasselmann et al. 1973). Even with present-day computing capabilities, a wave model based on the exact representation of nonlinear transfer is not feasible. Therefore, some form of parameterization of S_{nl} is needed. In WAM the Hasselmann et al. (1985) approximation is utilized.

The least-known source function is energy dissipation due to white capping. Hasselmann (1974) obtained some general constraints on the form of the dissipation source term, but a few parameters remained undetermined until Komen et al. (1984) insisted that for large time the wave spectrum would evolve towards the Pierson and Moskowitz (1964) spectrum. Felizardo and Melville (1995) found good agreement between dissipation rates of waves observed at sea and rates computed from the Komen et al. (1984) expression for S_{ds}.

WAM results are highly sensitive to the quality of the wind field. Manually analyzed winds have much lower errors compared to numerical weather prediction wind data products and, as a consequence, yield dramatically improved wave forecasts (Cardone et al. 1995). The sensitivity of modeled waves to the quality of the winds was confirmed by Janssen (1998), who showed that random wind speed errors dominate the forecast wave height error after day two in the forecast. It is shown in this paper that in the tropics, where sea state is dominated by swell, WAM depends on the quality of the wind field in the extratropics where swells are generated. Of course, this does not imply that there are no WAM errors; it means that WAM errors are smaller than the ones associated with the wind field. WAM errors can presumably be exposed only when the error in the wind field is reduced sufficiently, i.e., a reduction in wind speed error to 0.8 m s^{-1} (Janssen et al. 1997b).

Recent studies suggest that WAM may have a problem with swell energy. Sterl et al. (1998) found that WAM overpredicted swell wave height by about 20 cm. In contrast, Heimbach et al. (1998) found that WAM swell wave heights were lower than swell wave heights retrieved from synthetic aperture radar (SAR) data. However, Heimbach et al. (1998) used an operational ECMWF-WAM analysis that assimilated ERS-1 altimeter data, which underestimates wave height by 10–15% (Queffeulou 1996). In this paper, analyzed wave heights are shown to be sensitive to the quality of the altimeter wave height data used to produce the wave analysis.

The next section shows that relatively subtle changes in the wind may produce fairly considerable changes in systematic wave height forecast error.

2.2 ECMWF wave forecasting

Experimental wave forecasting with the initial version of WAM began at ECMWF in early 1987. Operational global sea state forecasting started at ECMWF in June 1992 with a 3°-latitude × 3°-longitude WAM. Shortly afterwards, a limited-area 0.5° × 0.5° WAM for the Mediterranean Sea was introduced. In August 1993, assimilation of ERS-1 altimeter wave height data commenced. Presently, global and limited-area versions of WAM simulations are computed at ECMWF.

The limited-area model, now called the European shelf model, covers the North Atlantic, North Sea, Baltic Sea, Mediterranean Sea, and Black Sea, and uses an irregular latitude-longitude grid with an approximately constant 28-km × 28-km resolution. The wave spectrum has 25 frequencies and 24 directions. Shallow-water effects, in particular bottom friction, are included.

The global WAM also has an irregular latitude-longitude grid with a 55-km grid spacing. The wave spectrum has 25 frequencies and 12 directions and shallow-water effects are included. In accord with Janssen (1989, 1991), WAM is now a component of the ECMWF operational atmospheric forecast-analysis system, with surface winds from the atmospheric general circulation model provided frequently to WAM. In addition, the sea-state dependent drag coefficient is determined with the stress induced by the ocean waves on the airflow. This two-way interaction of wind and waves yields a more consistent momentum budget at the ocean surface, producing a better balance between wind and waves. Presently, the operational atmospheric general circulation model has a T319 horizontal resolution and 31 layers in the vertical.

A sea-state drag coefficient has substantial impact on the forecast of a rapid developing, fast-moving atmospheric low pressure system. For example, the maximum difference in the minimum mean sea level pressures between a two-day forecast made with and without the sea-state dependent drag coefficient is 9 hPa for a North Pacific storm (Figure 1). Also, there is some impact on the 500-hPa geopotential height, and even at 200 hPa (Janssen and Viterbo 1996), indicating that ocean waves modify the momentum budget to produce a barotropic variation in the atmosphere. This example is exceptional because it shows a large-scale impact. Normally, as expected of physical processes near the surface, the impact on the atmosphere of two-way interaction is relatively small scale. In addition, extreme events are relatively rare.

Two-way interaction between wind and wave has considerable impact on forecasting surface wave height. For example, in the tropics, the mean forecast wave height error computed with (without) a sea-state dependent drag coefficient, decreased (increased)

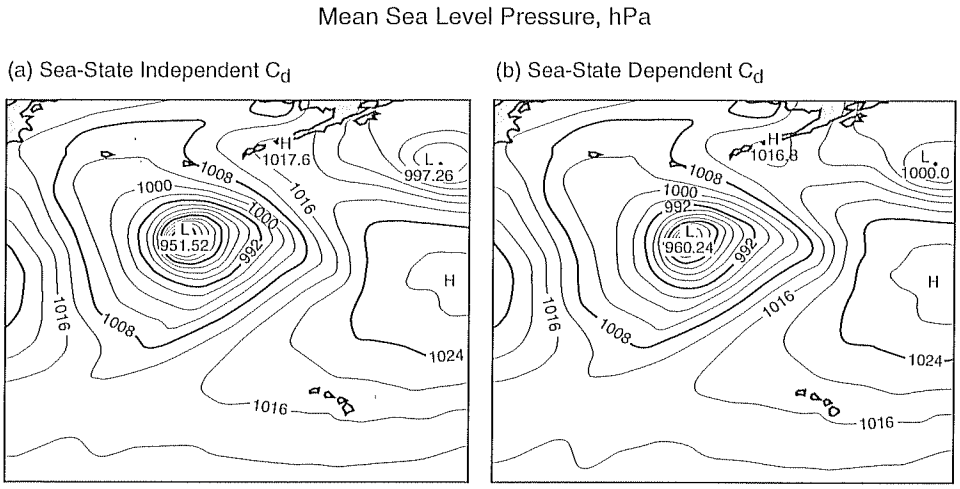

Figure 1. Two-day forecasts of mean sea level pressure made from initial conditions on 12 UT 12 December 1997 for (a) without sea-state dependent drag coefficient (C_d) i.e., without two-way interaction between wind and wave, and (b) with sea-state dependent C_d.

with forecast time (Figure 2). Having a sea-state dependent drag coefficient removes a long-standing problem of systematic forecast error growth in the ECMWF wave forecasting system. In 1994, systematic wave height errors in 5- to 10-day forecasts in the global 20°S–20°N tropical region were about 20% of the mean wave height. However, changes in the ECMWF atmospheric general circulation model in April 1995 (and continuing), and changes in the assimilation method for altimeter data in May 1996 reduced systematic errors to 5–10% of mean wave height. With introduction of an operational coupled atmosphere-ocean wave model at ECMWF on 29 June 1998, the systematic forecast error of wave height is 2–3% and has virtually disappeared.

The reduction of systematic forecast error of wave height in the tropics is an interesting problem because of the combination of local wind-generated waves, windsea, and remotely-forced wind-generated waves that have propagated long distances from the extratropics and are known as swell. In the tropics, swell is the main component of the sea state. In an atmospheric general circulation model, the momentum loss at the ocean surface is described by a drag coefficient. For a logarithmic wind profile, the drag coefficient, C_d, at height $z = L$ is

$$C_d = \left(\kappa / \ln \frac{L}{z_0}\right)^2 \tag{2}$$

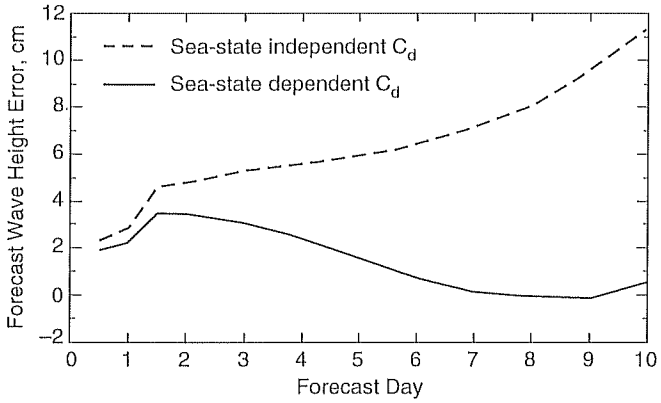

Figure 2. Ten-day forecasts of surface wave height error in the tropics (20°S–20°N, 360° longitudes), relative to the ECMWF verifying analysis, computed at 0.5-day intervals for 74 forecasts (16 April–28 June 1998) made with and without a sea-state dependent drag coefficient.

where κ is the von Karman constant and the roughness length z_0 is given by the Charnock (1955) relation,

$$z_0 = \frac{\alpha u_*^2}{g} \tag{3}$$

where u_* is the friction velocity, g is acceleration of gravity, and α is the Charnock parameter. In pre-June 1998 versions of the ECMWF atmospheric model with sea-state independent C_d, α has the constant value of 0.0185. With two-way interaction between wind and waves, the Charnock parameter is not constant but depends on sea state (Janssen 1991),

$$\alpha = 0.01\left(1 - \frac{\tau_w}{\tau}\right)^{-1/2} \tag{4}$$

where $\tau = \rho_a u_*^2$ is the total wind stress, ρ_a is the density of air at $z = L$, and τ_w is the wave-induced part of the total stress, which can be determined when the wind input source function S_{in} of the energy balance equation is known.

Young windseas, which are ocean waves just generated by wind, are usually steeper than old windseas (Hasselmann et al. 1973). For a young windsea, the contribution of the wave-induced stress to the total stress is larger than that for an old windsea, and the Charnock parameter will be larger than the nominal value of 0.0185 used in the pre-June 1998 ECMWF model. Therefore, a young windsea reduces the strength of the surface wind.

Consequently, wave heights computed from the extratropical wind field with a sea-state dependent C_d will be reduced and systematic forecast wave height error will be lower compared to those computed with the constant Charnock parameter (Janssen and Viterbo 1996). Improved forecasting of extratropical wave heights produces better estimates of swell propagating through the tropics, which reduces the forecast error of wave height in the tropics. However, the treatment of swell is not fully solved as Sterl et al. (1998) suggested that the propagation of wave energy is in error. But the quality of the ECMWF wind field improved as well with the implementation of two-way wind-wave interaction in the ECMWF forecast-analysis system on 29 June 1998. The root-mean-square (rms) difference computed between the ECMWF 6-hour and ERS-2 scatterometer winds shows that a 20 cm s^{-1} (about 10% of total error) reduction occurred on 29 June 1998 (Figure 3). The bias is reduced by about the same amount, although not as clearly visible in Figure 3.

2.3 Future developments

Beginning in 1993, ECMWF started ensemble forecasting to obtain information on the uncertainty of the deterministic forecast, and ensemble prediction of ocean waves began 29 June 1998. The present ensemble prediction system consists of the coupling of the ECMWF T159 atmosphere model and the 1.5° × 1.5° WAM. The ensemble consists of 50 members which are generated by perturbing the deterministic atmospheric analysis by the most unstable singular vectors. Preliminary results (not shown) indicate a promising future for probabilistic forecasting of waves.

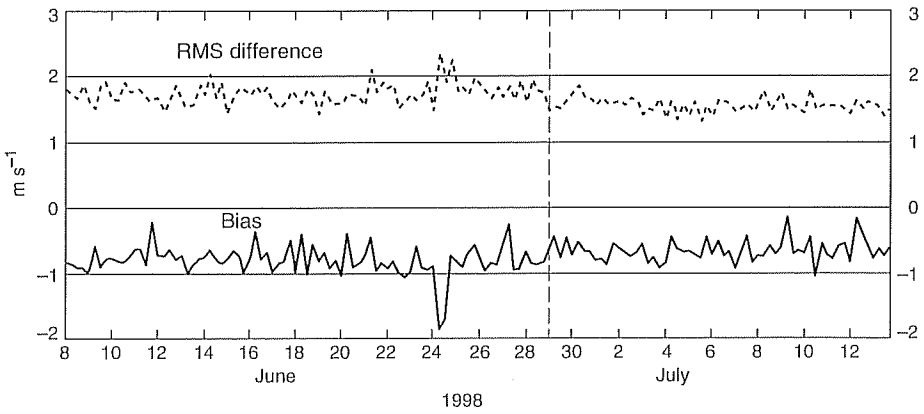

Figure 3. Bias (ERS-2 minus ECMWF) and rms difference between 6-h ECMWF surface wind data product and ERS-2 scatterometer wind measurements.

An important aspect of wave forecasting is the ability to predict extreme events associated with hurricanes and extratropical storms. However, numerical weather prediction models have difficulty simulating the wind field because of lack of horizontal resolution and inaccurate representation of physical processes. In recent years, considerable progress occurred on increasing model resolution and model parameterization of sub-grid-size-scale atmospheric dynamical processes. For example, the operational 36-h forecast of Hurricane Luis (initial conditions on 9 September 1995) in its extratropical phase south of Nova Scotia, Canada, is compared with a 36-h forecast made with the current system. In the current system, the experimental forecast was generated with the four-dimensional variational system, while the operational forecast was based on optimum interpolation. Operational (T213 resolution) and experimental (T639 resolution) forecasts of minimum sea level pressures were 977 and 963 hPa, respectively. According to the National Oceanic and Atmospheric Administration (NOAA) National Hurricane Center, the observed minimum sea level pressure was 965 hPa, which was only 2 hPa higher than that computed with the recent ECMWF system but 12 hPa lower than the value predicted with the operational system in use at ECMWF in September 1995. The newer version of the ECMWF forecast-analysis system not only gives a much deeper atmospheric low pressure, but also the location of the low is in better agreement with observations. The consequences for wave prediction are remarkable (Figure 4). Maximum wave height recorded at a NOAA buoy was 17 m, which was about 30 cm off the prediction from the newer ECMWF system but nearly 7 m different than predicted with the old operational system. An attempt was made to examine reasons for the large differences in the simulation of Hurricane Luis. The change of data assimilation method from optimal interpolation to

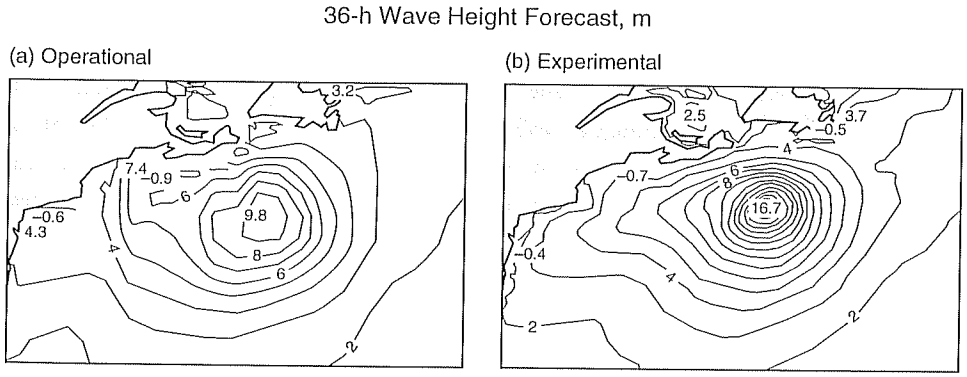

Figure 4. Thirty-six-hour wave height forecasts made with two different ECMWF forecast-analysis systems: (a) T213 operational system of 9 September 1995, named Operational, and (b) T639 system, named Experimental. Initial conditions were at 12 UT 9 September 1995.

four-dimensional variation resulted in a relatively minor improvement of forecast wave height. The relative insensitivity of forecast maximum wave height to the change of assimilation method is not typical, and is probably related to the particular circumstance that the atmospheric low was small scale, while the present version of the variational assimilation method affects relatively large scales. Improvements in wave forecasts due to changes within the atmospheric general circulation model, including horizontal and vertical resolutions, are more dramatic. The most likely candidate for the better forecast is the improved representation of convection (A. Beljaars, private communication 1999), which was introduced into the operational ECMWF system at the end of 1997. Recent changes in the semi-Lagrangian scheme may also have contributed to the improvement. The experimental simulation of Hurricane Luis (not shown) suggests that the present T319 resolution is adequate for small-scale extreme events. The future appears even more promising because in a couple of years a further increase is expected in the horizontal resolution of the ECMWF operational atmospheric general circulation model.

3. Altimeter Wave Height

3.1 ERS-2 data

A numerical weather prediction center, such as ECMWF, requires satellite observations within three hours after the remote-sensed observations have been made in order to assimilate the data into the operational forecast-analysis system. For ERS-1/2, quasi-real-time data products are Fast Delivery products.

Numerical weather prediction data products are quite useful to validate and calibrate satellite data products. For example, just after the launch of ERS-1, the altimeter global mean wave height was about 1-m higher than that simulated with the ECMWF model. Investigation of the detected bias led to the discovery of a small offset in the pre-launch instrument characterization data. When the processing algorithm was updated at all ground stations, the ERS-1 altimeter wave height was found to be satisfactory. The ERS-2 altimeter wave heights showed, from the first day onwards, a remarkably good agreement with the ECMWF 6-h wave height, except at low wave height where ERS-2 had a higher cut-off value than ERS-1. This higher cut-off value is caused by the somewhat different instrumental specifications of the ERS-2 altimeter. Because ERS-2 was launched while ERS-1 was still operational, a comparison of ERS-1 and ERS-2 wave heights revealed that ERS-2 altimeter wave heights were 8% higher than those from ERS-1. This difference was regarded as favorable because ERS-1 wave heights underestimated buoy data (Janssen et al. 1997a). Since the altimeters on ERS-1 and ERS-2 use the same wave height algorithm, the improved performance of the ERS-2 altimeter (Janssen et al. 1997a) is probably related to a different data processing procedure. Indeed, the ERS-2 data processor uses a

more accurate procedure to obtain the wave form, which results in better estimation of wave height.

In-situ (NOAA buoys) and ERS altimeter wave heights are used to validate the ECMWF wave forecasting system. The monthly mean bias between ECMWF and buoy wave heights in the Northern Hemisphere was about 25 cm during ERS-1 (Figure 5), became virtually zero during the summer months of 1996 (at the beginning of ERS-2), and then was 15 cm during autumn 1996 (Figure 5). With the introduction of ERS-2 wave height data, the bias during the Northern Hemisphere summer, in which the sea state is characterized by swell and windsea of low steepness, is removed, but the ECMWF wave product still underestimates buoy wave height during the following winter (Figure 5), when the sea state has a considerable fraction of windsea with large steepness. It could be argued that the ECMWF wave forecasting system is underestimating windsea wave height. However, the ERS-2 altimeter wave height was less than the buoy data (Figure 6) by about 22 cm or 7%, with an rms difference of 47 cm.

The satellite altimeter wave height retrieval depends in a sensitive manner on the procedure how to obtain the slope of the wave form, and this could, at least to some extent, explain the discrepancy between altimeter wave height and buoy wave height. However, it does not explain why in cases of swell the altimeter performs better. This led us to suspect that perhaps there are problems with the retrieval of altimeter wave height in cases of large steepness, because most wave height algorithms assume that wave height and steepness distributions are Gaussian, which for large steepness, when nonlinear effects become important, may not be valid. It would thus be natural to study the dependence of altimeter wave height error on ocean wave steepness. However, if buoy observations are used as truth, a few years of collocated data are needed to obtain statistically significant results. Using an ECMWF data product as truth requires, however, only a month of collocations, since there are typically about 40,000 collocations between altimeter and ECMWF-modeled wave heights during one month. Hence, we used the ECMWF 6-h wave heights as truth. For relatively small slopes when swells dominate the sea state, the ERS-2 altimeter

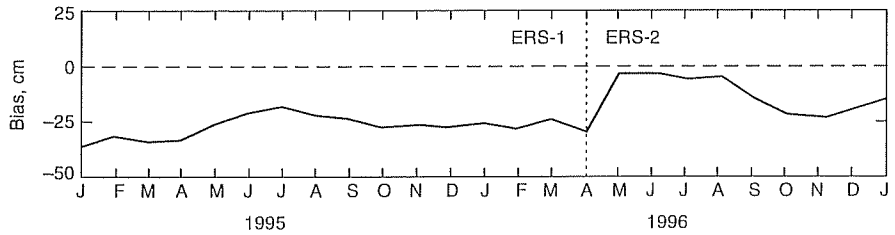

Figure 5. Bias (ECMWF minus buoy) between ECMWF modeled wave height and moored-buoy wave height measurements in the North Atlantic and North Pacific.

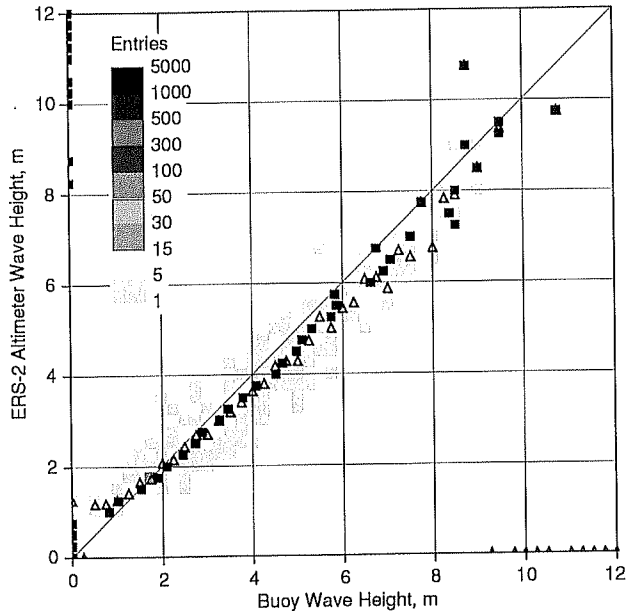

Figure 6. Scatter diagram of mean values of 0.25-m binned moored-buoy and ERS-2 altimeter wave heights for February 1997 for buoy data in the North Atlantic and North Pacific. Solid squares (open triangles) denote mean buoy (altimeter) wave height versus binned altimeter (buoy) wave height. Color code denotes the number of collocations.

wave height error is small; for large slopes, the altimeter underestimates wave height by as much as 50 cm (Figure 7). The next section describes the role of nonlinearity in the retrieval of wave height from the altimeter wave form.

3.2 Electromagnetic bias and altimeter retrieval algorithm

The average radar cross section for backscatter of randomly distributed specular points in the rough surface approximation (Barrick 1972; Barrick and Lipa 1985) is a function of time because contributions from ocean wave crests arrive at the altimeter before those from wave troughs. The time-dependent cross section is called the wave form. For a nadir-scanning radar, the wave form depends on the joint probability distribution (jpd) of surface elevation and surface slope under the condition of zero mean slope. In order to obtain a practical altimeter retrieval algorithm, the probability distributions of the surface elevation and slope are each assumed to have a Gaussian shape, which is reasonable for weakly nonlinear ocean waves (Longuet-Higgins 1963). Although this yields

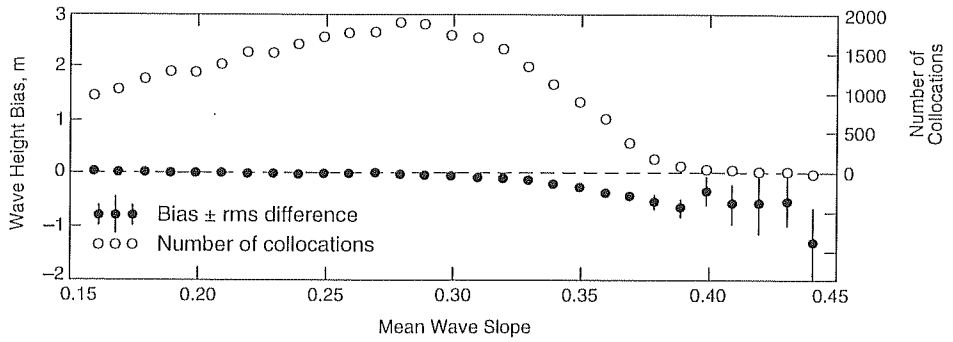

Figure 7. Wave height bias (altimeter minus ECMWF 6 h) computed at 0.01 increments of wave slope for February 1997.

good estimates for altimeter wave height, the Gaussian assumption does not include a weak, nonlinear wave process that affects the altimeter range measurement, known as electromagnetic bias (EMB), which is caused by waves having a sharp crest and a wide trough. An altimeter retrieval algorithm without consideration of EMB would emphasize the part of the sea surface below mean sea level, and, therefore, the altimeter range measurement would estimate a somewhat longer distance between satellite and ocean surface. For linear waves with small steepness the Gaussian probability distribution is valid and EMB vanishes. Also, waves may distort the altimeter pulse to produce an additional error in the altimeter range measurement of the height of the satellite above the sea surface; this error is called the instrumental error. The sum of instrumental error and electromagnetic bias is called the sea state bias (SSB).

Deviations from the Gaussian distribution may occur for a number of reasons, and we explore the consequences of a nonlinear wave surface with sharp crests and wide troughs, i.e., EMB, on altimeter retrieval of wave height. For a radar pulse with Gaussian shape and width, ν, Srokosz (1986) showed that the wave form, W, is

$$W \sim \frac{1}{2}\left[1 + erf(T) + \frac{e^{-\frac{T^2}{2}}}{\sqrt{\pi}}\left\{\frac{\lambda\sqrt{2}}{3}(1+T^2) - \frac{1}{\sqrt{2}}(\lambda+\delta)\right\}\right] \tag{5}$$

where $erf(T)$ is the error function, c is the speed of light, H_s is the significant wave height, T is the normalized time $\frac{t}{t_p}$, and

$$t_p = \frac{2}{c}\sqrt{v^2 + \frac{1}{8}H_s^2} \tag{6}$$

Deviations from a Gaussian distribution are measured by the skewness factor, λ, and the elevation-slope correlation, δ, which depend in a complicated way on the wave spectrum (Longuet-Higgins 1963; Jackson 1979). Using the Phillips (1958) spectrum

$$F(k) = \frac{1}{2}\alpha_p k^{-3} \tag{7}$$

then

$$\delta = 2\lambda \qquad \lambda = 2\sqrt{\alpha_p} \tag{8}$$

where α_p is the Phillips parameter, and, as noted by Srokosz (1986), λ is corrected by a factor two compared to that obtained by Longuet-Higgins (1963). Swell has typically a smaller Phillips parameter by a factor of 4–10 than windsea; therefore, swell has in practice a Gaussian distribution, while windsea, with α_p approximately equal to 0.01, may show considerable deviations from a Gaussian distribution.

The half-power of a radar pulse wave form, W, with a Gaussian jpd occurs at the origin, $T = 0$ (Figure 8), which corresponds to mean sea level. For a Gaussian jpd, EMB vanishes, and only the first two terms in equation (5) remain. H_s is determined from the half-power wave form slope, s,

$$H_s = 4\left(\frac{\kappa_1}{s^2} - \kappa_2\right)^{1/2} \tag{9}$$

where κ_1 and κ_2 depend on the power and width of the transmitted pulse and on the speed of light.

For a non-Gaussian jpd, the half-power point of the wave form (equation (5)) is shifted towards positive time (Figure 8) because in the presence of weakly nonlinear waves the radar altimeter range measurement overestimates the distance between mean surface and satellite. H_s is also determined by the half-power slope, which, however, does not coincide with $T = 0$. Assuming small deviations from a Gaussian distribution, i.e., λ and δ are small, an approximate expression for the observed H_s is

$$H_s = 4\left(\frac{\kappa_3}{s^2} - \kappa_2\right)^{1/2} \tag{10}$$

and

$$\kappa_3 = \kappa_1\left(1 + 2\left(\frac{\lambda}{3} + \delta\right)\left(\frac{5}{24}\lambda + \frac{1}{8}\delta\right)\right) \tag{11}$$

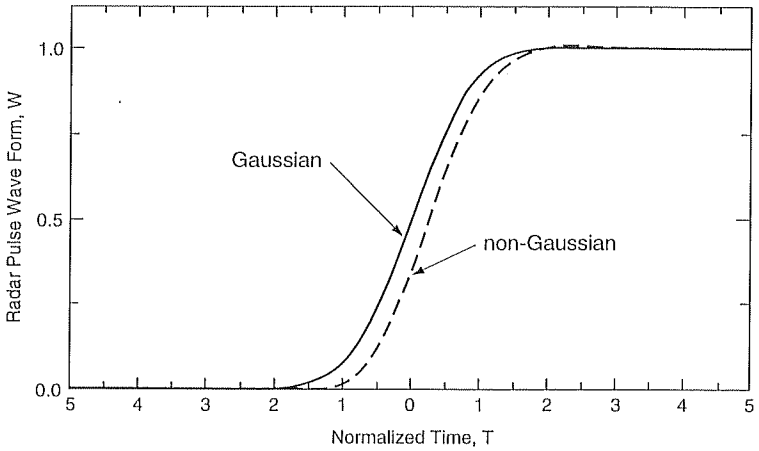

Figure 8. Distribution of radar pulse wave form, *W*, with normalized time, *T*, for Gaussian and non-Gaussian joint probability distributions of wave height and slope.

The EMB correction to the altimeter range measurement is

$$\mathrm{EMB} = -\frac{1}{8}\left(\frac{\lambda}{3} + \delta\right) H_S \tag{12}$$

For the Phillips spectrum defined by equation (7), then

$$\kappa_3 = \kappa_1\left(1 + \frac{154}{18}\alpha_p\right) \tag{13}$$

and

$$\frac{\mathrm{EMB}}{H_s} = -\frac{7}{12}\sqrt{\alpha_p} \tag{14}$$

Deviations from a Gaussian distribution produce a modest impact on altimeter wave height retrieval because the correction depends on α_p, which is, in the extreme condition of young windsea, at most 0.025; thus, at the maximum, the correction to wave height would be 10%. EMB may vary by a factor of two to three, depending on sea state, being small for swell and large for a young windsea (Minster et al. 1992).

WAM spectra are used to determine λ and δ, and, consequently, EMB. The chosen period was February 1997, when a number of extreme events occurred in the North Atlantic. EMB corrections were applied to the ERS-2 Fast Delivery altimeter data. The corrected altimeter wave heights are in slightly better agreement with buoy data. The bias

has been reduced from 22 cm (Figure 6) to 14 cm (Figure 9), i.e., the mean corrected wave height is about 3% larger. The rms difference between corrected ERS-2 wave heights and buoy data is 46 cm and is the same as that computed with uncorrected ERS-2 data. This is a disappointing result, but it should be realized that in deriving the correction for wave height, we have assumed that wave height was obtained from the half-power slope of the wave form. This is not the ESA procedure to obtain the Fast Delivery wave height (R. Francis, private communication 1997). Further tests are warranted because the impact of the nonlinear sea state on wave height retrieval is sensitive to the procedure of how to obtain the slope of the wave form.

Comparison of the EMB correction computed from WAM spectra and the SSB correction computed from ERS-2 data by the Gaspar and Ogor (1996) method showed fair agreement and remarkable differences (Figure 10). For low values of EMB and SSB, EMB is too low compared to SSB, while for large corrections, the opposite is found. Realizing that to first approximation, EMB depends linearly on wave height, it is concluded that for low wave height, i.e., swell conditions, the WAM approach underestimates

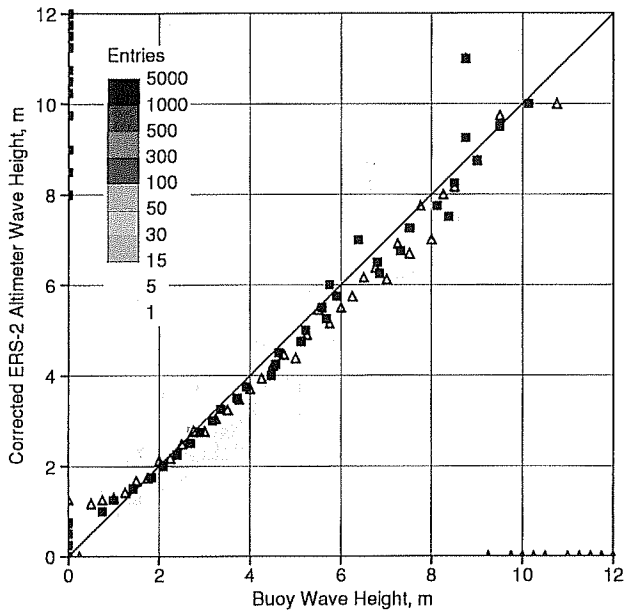

Figure 9. Scatter diagram of mean values of 0.25-m binned moored-buoy and nonlinear-corrected ERS-2 altimeter wave heights for February 1997 for buoy data in the North Atlantic and North Pacific. Solid squares (open triangles) denote mean buoy (altimeter) wave height versus binned altimeter (buoy) wave height. Color code denotes the number of collocations.

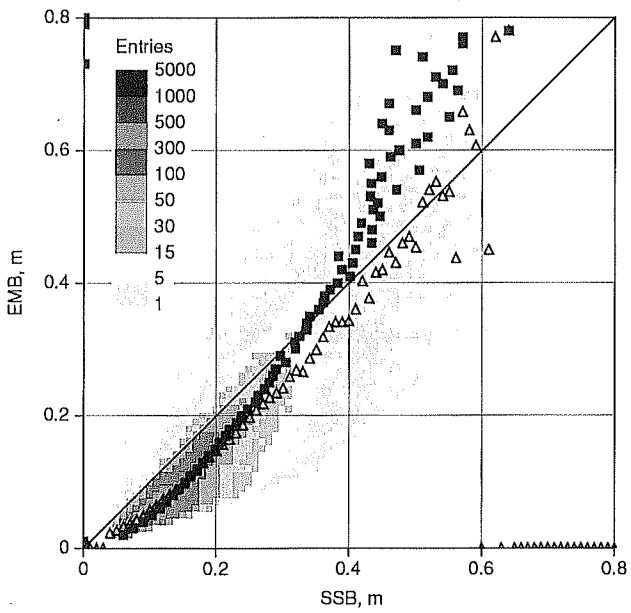

Figure 10. Scatter diagram of WAM-derived electromagnetic bias (EMB), according to the Srokosz (1986) method, and ERS-2 sea state bias (SSB), according to the Gaspar and Ogor (1996) method. Global data for February 1997 were used. Color code denotes the number of collocations.

SSB, but for windseas, the WAM method seems to give reasonable estimates of SSB. According to equation (14), EMB is lower for swell than for windsea.

The question, why the ERS-derived SSB has little sea-state dependency, is examined with reference to the dimensionless wave height, gH_s / U_{10}^2 (where U_{10} is wind speed at 10-m height), which is a measure of wave development. For an old windsea, the dimensionless wave height is about 0.25; a young windsea has smaller values and swell has larger values. The WAM-derived EMB has a much greater sensitivity to the dimensionless wave height compared to SSB computed from ERS-2 data with the Gaspar and Ogor (1996) method (Figure 11). A direct estimate of EMB is found in Melville et al. (1991), which shows a clear sea-state dependence with dimensionless wave height (Figure 11). There is a fair agreement with the WAM-derived EMB. Perhaps, the absence of sea-state dependency of the Gaspar and Ogor (1996) SSB is caused by the instrumental error having an effect opposite to that created by the EMB, but it is evident that more research is needed to clarify this issue.

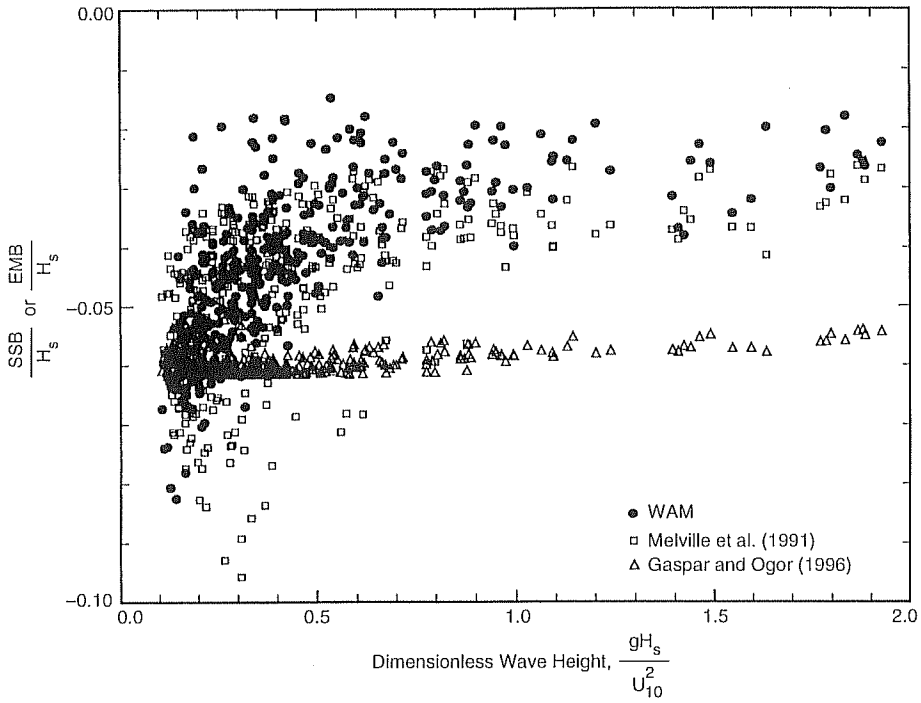

Figure 11. Scatter diagram between the dimensionless wave height and WAM-derived EMB, EMB computed from the Melville et al. (1991) formulation, and SSB computed in accord with Gaspar and Ogor (1996). Each bias is relative to ERS-2 measurements of H_s during February 1997. The 10-m height wind speed was computed from ERS-2 altimeter data.

4. Conclusions

Considerable progress has been made in the past twenty years in wave modeling and in satellite wind and wave products. The combined use of satellite and wave model products has also revealed problems. There may a problem in how WAM treats swell, although presently it is not clear whether there is too much swell or not enough. There may be a problem with the altimeter wave height retrieval for young, nonlinear sea states. Finally, two-dimensional WAM spectra may provide information on EMB. Further studies are planned to resolve some of the issues mentioned in this paper.

Acknowledgments. The author acknowledges the support by the members of the ECMWF wave group Jean Bidlot, Björn Hansen and Martin Hoffschildt. Furthermore, useful discussions with members of ESA's Altimeter Scientific Advisory Group Johnny Johannessen, Richard Francis, Remko Scharroo, Seymoor Laxon and Monica Roca are very much appreciated. I thank Lars Isaksen for providing Figure 3, whilst stimulating discussions with Martin Miller are gratefully acknowledged as well. Two reviewers are thanked for their comments, which improved the paper.

References

Anctil, F., and M. A. Donelan, Air-water momentum flux observations over shoaling waves, *J. Phys. Oceanogr.*, *26*, 1344–1353, 1996.

Barrick, D. E., Remote sensing of sea state by radar, In Remote Sensing of the Troposphere, edited by V. E. Derr, U. S. Govt. Printing Office, Washington, D.C., 12-1 to 12-46, 1972.

Barrick, D. E., and B. Lipa, Analysis and interpretation of altimeter sea echo, *Adv. Geophys.*, *27*, 60–99, 1985.

Bauer, E., S. Hasselmann, K. Hasselmann, and H. C. Graber, Validation and assimilation of Seasat altimeter wave heights using the WAM wave model, *J. Geophys. Res.*, 12671–12682, 1992.

Bauer, E., and C. Staabs, Statistical properties of global significant wave heights and their use for validation, *J. Geophys. Res.*, *103*, 1153–1166, 1998.

Cardone, V. J., H. C. Graber, R. E. Jensen, S. Hasselmann, and M. J. Caroso, In search of the true surface wind field in SWADE IOP-1: Ocean wave modeling perspective, *Global Atmos. Ocean Sys.*, *3*, 107–150, 1995.

Charnock, H., Wind stress on a water surface, *Quart. J. Roy. Meteorol. Soc.*, *81*, 639–640, 1955.

Donelan, M. A., The dependence of the aerodynamic drag coefficient on wave parameters, In Proc. First International Conference on Meteorological and Air/Sea Interaction of the Coastal Zone, Amer. Meteorol. Soc., Boston, 381–387, 1982.

Donelan, M. A., F. W. Dobson, S. D. Smith, and R. J. Anderson, On the dependence of sea surface roughness on wave development, *J. Phys. Oceanogr.*, *23*, 2143, 1993.

Felizardo, F. C., and W. K. Melville, Correlations between ambient noise and the ocean surface wave field, *J. Phys. Oceanogr.*, *25*, 513–532, 1995.

Gaspar, P., and F. Ogor, Estimation and analysis of the sea state bias of the new ERS-1 and ERS-2 altimetric data (OPR version 6), Tech. Rep. CLS/DOS/NT/96.041, Collect. Localisation, Satell. Agne, Toulouse, France, 1996.

Gelci, R., H. Cazale, and J. Vassal, Prevision de la houle: La methode des densites spectroangulaires, *Bull. Inform. Comité Central Oceanogr. Etudes Côtes*, *9*, 416–435, 1957.

Hansen, B., and H. Guenther, ERS-1 radar altimeter validation with the WAM model, In Proc. ERS-1 Geophysical Validation Workshop, European Space Agency, Paris, 157–161, 1992.

Hare, J. E., P. O. G. Persson, C. W. Fairall, and J. B. Edson, Behaviour of Charnock's relation for high wind conditions, In Proc. 13th AMS Conference on Boundary Layers and Turbulence, Amer. Meteorol. Soc., Boston, 252–255, 1999.

Hasselmann, K., On the non-linear energy transfer in a gravity-wave spectrum: General theory, *J. Fluid Mech.*, *12*, 481–500, 1962.

Hasselmann, K., On the spectral dissipation of ocean waves due to white capping, *Bound. Layer. Meteorol.*, *6*, 107–127, 1974.

Hasselmann, K., T. P. Barnett, E. Bouws, H. Carlson, D. E. Cartwright, K. Enke, J. A. Ewing, H. Gienapp, D. E. Hasselmann, P. Kruseman, A. Meerburg, P. Mueller, D. J. Olbers, K. Richter, W. Sell, and H. Walden, Measurements of wind-wave growth and swell decay during the Joint North Sea Wave Project (JONSWAP), *Deuts. Hydrogr. Z. Suppl.*, *A8*, 1–95, 1973.

Hasselmann, S., and K. Hasselmann, Computations and parameterisations of the nonlinear energy transfer in a gravity-wave spectrum: A new method for efficient computations of the exact nonlinear transfer integral, *J. Phys. Oceanogr.*, *15*, 1369–1377, 1985.

Heimbach, P., S. Hasselmann, and K. Hasselmann, Statistical analysis and intercomparison of WAM model data with global ERS-1 SAR wave mode spectral retrievals over 3 years, *J. Geophys. Res.*, *103*, 7931–7977, 1998.

Jackson, F. C., The reflection of impulses from a nonlinear random sea, *J. Geophys. Res.*, *84*, 4939–4943, 1979.

Janssen, J. A. M., Does wind stress depend on sea-state or not? A statistical error analysis of HEXMAX data, *Bound. Layer. Meteorol.*, *83*, 479–503, 1997.

Janssen, P. A. E. M., Wave-induced stress and the drag of air flow over sea waves, *J. Phys. Oceanogr.*, *19*, 745–754, 1989.

Janssen, P. A. E. M., Quasi-linear theory of wind-wave generation applied to wave forecasting, *J. Phys. Oceanogr.*, *21*, 1631–1642, 1991.

Janssen, P. A. E. M., On error growth in wave models, ECMWF Tech. Memo 249, European Centre for Medium-Range Weather Forecasts, Reading, United Kingdom, 12 pp, 1998.

Janssen, P. A. E. M., P. Lionello, M. Reistad, and A. Hollingsworth, Hindcasts and data assimilation studies with the WAM model during the Seasat period, *J. Geophys. Res.*, *94*, 973–993, 1989.

Janssen, P. A. E. M., and P. Viterbo, Ocean waves and the atmospheric climate, *J. Climate*, *9*, 1269–1287, 1996.

Janssen, P. A. E. M., B. Hansen, and J. Bidlot, Validation of ERS satellite wave products with the WAM model, In CEOS Wind and Wave Validation Workshop Report, ESA WPP147, ESTEC, The Netherlands, 101–108, 1997a.

Janssen, P. A. E. M., B. Hansen, and J.-R. Bidlot, Verification of the ECMWF wave forecasting system against buoy and altimeter data, *Wea. Forecasting*, *12*, 763–784, 1997b.

Johnson, H. K., J. Hojstrup, H. J. Vested, and S. Larson, On the dependence of sea surface roughness on wind waves, *J. Phys. Oceanogr.*, *28*, 1702–1716, 1998.

Khandekar, M. L., and R. Lalbeharry, An evaluation of Environment Canada's operational wave model based on moored buoy data, *Wea. Forecasting*, *11*, 139–152, 1996.

Komen, G. J., L. Cavaleri, M. Donelan, K. Hasselmann, S. Hasselmann, and P. A. E. M. Janssen, editors, *Dynamics and Modelling of Ocean Waves*, Cambridge University Press, Cambridge, 532 pp, 1994

Komen, G. J., K. Hasselmann, and S. Hasselmann, On the existence of a fully developed windsea spectrum, *J. Phys. Oceanogr.*, *14*, 1271–1285, 1984.

Lionello, P., H. Günther, and P. A. E. M. Janssen, Assimilation of altimeter data in a global ocean wave model, *J. Geophys. Res.*, *97*, 14453–14474, 1992.

Lipa, B., and D. E. Barrick, Ocean surface height-slope probability density function from SEASAT altimeter echo, *J. Geophys. Res.*, *86*, 10921–10930, 1981.

Longuet-Higgins, M. S., The effect of nonlinearities on statistical distributions in the theory of sea waves, *J. Fluid Mech.*, *17*, 459–480 1963.

Melville, W. K., R. H. Stewart, W. C. Keller, J. A. Kong, D. V. Arnold, A. T. Jessup, M. R. Loewen, and A. M. Slinn, Measurements of electromagnetic bias in radar altimetry, *J. Geophys. Res.*, *96*, 4915–4924, 1991.

Miles, J. W., On the generation of surface waves by shear flows, *J. Fluid Mech.*, *3*, 185–204, 1957.

Minster, J. F., D. Jourdan, Ch. Boissier, and P. Midol-Monnet, Estimation of the sea-state bias in radar altimeter GEOSAT data from examination of frontal systems, *J. Atmos. Oceanic Tech.*, *9*, 174–187, 1992.

Mitsuyasu, H., On the growth of the spectrum of wind-generated waves: 1, Rep. Res. Inst. Appl. Mech., Kyushu Univ., *16*, 251–264, 1968.

Mitsuyasu, H., On the growth of the spectrum of wind-generated waves: 2, Rep. Res. Inst. Appl. Mech., Kyushu Univ., *17*, 235–243, 1969.

Monbaliu, J., On the use of the Donelan wave spectral parameter as a measure for the roughness of wind waves, *Bound. Layer. Meteorol.*, *67*, 277–291, 1994.

Pierson, W. J., G. Neumann, and R. W. James, Practical Methods for Observing and Forecasting Ocean Waves by Means of Wave Spectra and Statistics, H.O. Pub 603, U.S. Navy Hydrographic Office, Washington, D.C., 284 pp, 1955.

Pierson, W. J., Jr,. and L. Moskowitz, A proposed spectral form for fully developed wind-seas based on the similarity theory of S. A. Kitaigorodskii, *J. Geophys. Res.*, *69*, 5181, 1964.

Phillips, O. M., On the generation of waves by turbulent wind, *J. Fluid Mech.*, *2*, 417–445, 1957.

Phillips, O. M., The equilibrium range in the spectrum of wind-generated waves, *J. Fluid Mech.*, *4*, 426–434, 1958.

Phillips, O. M., The dynamics of unsteady gravity waves of finite amplitude: 1, *J. Fluid Mech.*, *9*, 193–217, 1960.

Queffelou, P., Significant wave height and backscatter coefficient at ERS-1/2 and Topex/Poseidon ground track crossing points, FDP, IFREMER contribution to the ERS-2 radar altimeter commissioning phase, IFREMER Tech Rep., IFREMER, DRP/OS, BP 70, Plouzane, France, 25 pp, 1996.

Romeiser, R., Global validation of the wave model WAM over a one year period using Geosat wave height data, *J. Geophys. Res.*, *98*, 4713–4726, 1993.

Smith, S. D., R. J. Anderson, W. A. Oost, C. Kraan, N. Maat, J. DeCosmo, K. B. Katsaros, K. L. Davidson, K. Bumke, L. Hasse, and H. M. Chadwick, Sea surface wind stress and drag coefficients: The HEXOS results, *Bound. Layer. Meteorol.*, *60*, 109–142, 1992.

Snyder, R. L., F. W. Dobson, J. A. Elliot, and R. B. Long, Array measurements of atmospheric pressure fluctuations above surface gravity waves, *J. Fluid Mech.*, *102*, 1–59, 1981.

Srokosz, M. A., On the joint distribution of surface elevation and slope for a nonlinear random sea, with application to radar altimetry, *J. Geophys. Res.*, *91*, 995–1006, 1986.

Sterl, A. G., G. J. Komen, and P. D. Cotton, Fifteen years of global wave hindcasts using ERA winds: Validating the reanalysed winds and assessing the wave climate, *J. Geophys. Res.*, *103*, 5477–5492, 1998.

Sverdrup, H. U., and W. H. Munk, Wind Sea and Swell: Theory of Relations for Forecasting, H.O. Pub. 601, U.S. Navy Hydrographic Office, Washington, D.C., 44 pp, 1947.

SWAMP Group: J. H. Allender, T. P. Barnett, L. Bertotti, J. Bruinsma, V. J. Cardone, L. Cavaleri, J. Ephraums, B. Golding, A. Greenwood, J. Guddal, H. Gunther, K. Hasselmann; S. Hasselmann, P. Joseph, S. Kawai, G. J. Komen, L. Lawson, H. Linne, R. B. Long, M. Lybanon, E. Maeland, W. Rosenthal, Y. Toba, T. Uji, and W. J. P. de Voogt, *Sea Wave Modeling Project (SWAMP): An Intercomparison Study of Wind Wave Prediction Models, Part 1: Principal Results and Conclusions*, Plenum, New York, 256 pp, 1985.

WAMDI Group: S. Hasselmann, K. Hasselmann, E. Bauer, P. A. E. M. Janssen, G. J. Komen, L. Bertotti, P. Lionello, A. Guillaume, V. C. Cardone, J. A. Greenwood, M. Reistad, L. Zambresky, and J. A. Ewing, The WAM model: A third generation ocean wave prediction model, *J. Phys. Oceanogr.*, *18*, 1775–1810, 1988.

Wittmann, P. A., R. M. Clancy, and T. Mettlach, Operational wave forecasting at Fleet Numerical Meteorology and Oceanography Center, Monterey, CA., In Fourth Int. Workshop on Wave Hindcasting and Forecasting, Atmospheric Environment Service, Ottawa, 335–342, 1995.

Yelland, M. J., B. I. Moat, P. K Taylor, R. W. Pascal, J. Hutchings, and V. C. Cornell, 1998. Wind stress measurements from the open ocean corrected for airflow distortion by the ship, *J. Phys. Oceanogr.*, *28*, 1511–1526, 1998.

Zambresky, L., A verification study of the global WAM model, December 1987–November 1988, ECMWF Tech. Rep. 63, European Centre for Medium-Range Weather Forecasts, Reading, United Kingdom, 86 pp, 1989.

Peter Janssen, European Centre for Medium-Range Weather Forecasts (ECMWF), Shinfield Park, Reading RG2 9AX, United Kingdom. (email, peter.janssen@ecmwf.int;fax, +44-118-986-9450)